Bone 127 (2019) 260–270

Contents lists available at ScienceDirect

Bone

journal homepage: www.elsevier.com/locate/bone

Full Length Article

The longitudinal effects of ovariectomy on the morphometric, densitometric and mechanical properties in the murine tibia: A comparison between two mouse strains

Bryant C. Roberts[a,b,1], Mario Giorgi[a,c,1], Sara Oliviero[a,b], Ning Wang[a,d], Maya Boudiffa[a,d], Enrico Dall'Ara[a,b,d,*]

[a] Department of Oncology and Metabolism, University of Sheffield, Sheffield, UK
[b] Insigneo Institute for in silico Medicine, University of Sheffield, Sheffield, UK
[c] Certara QSP, Certara UK Ltd., Simcyp Division, Sheffield, UK
[d] MRC Arthritis Research UK Centre for Integrated research into Musculoskeletal Ageing (CIMA), University of Sheffield, Sheffield, UK

ARTICLE INFO

Keywords:
Ovariectomy
In vivo microCT
Bone morphometry
Bone densitometry
Mechanical properties

ABSTRACT

Oestrogen deficiency-related bone loss in the ovariectomized (OVX) mouse is a common model for osteoporosis. However, a comprehensive in vivo assessment of intervention-related changes in multiple bone properties, and in multiple mouse strains, is required in order to identify an appropriate model for future evaluation of novel anti-osteoporotic therapies. The aim of this study was to evaluate the effect of OVX on the morphometric and densitometric properties measured in the microCT images and the mechanical properties estimated with finite element models of the tibia in two mouse strains, C57BL/6 and BALB/c.

14-weeks-old female C57BL/6 and BALB/c mice were divided into two groups per strain: (1) ovariectomized, (2) non-operated control. The right tibia was scanned at baseline (14 weeks) and then every two weeks thereafter, until 24-weeks-old, using in vivo microCT. Changes in trabecular and cortical bone morphometry, spatiotemporal changes in densitometric properties and in mechanical properties (from micro-finite element (μFE) analysis) were computed. Differences between OVX and non-operated controls were evaluated by ANCOVA, adjusted for 14-weeks baseline.

In morphometry, trabecular bone mass was significantly reduced in both C57BL/6 and BALB/c from four weeks following surgery. Though the OVX-effect was transient in BALB/c as bone mass reached skeletal homeostasis. OVX inhibited the age-related thickening of cortical bone only in C57BL/6. In both strains, increments in bone mineral content were significantly lower with OVX only in the proximal tibia, with intervention-related differences increasing with time. OVX had no effect on μFE estimates of stiffness nor failure load in either strain.

The results of this study show strain-, time- and region-(trabecular or cortical) dependent changes in morphometric and densitometric properties. These findings highlight the importance of choosing an appropriate mouse model and time points for research of treatments against accelerated bone resorption.

1. Introduction

Osteoporosis (OP) and associated fractures are major clinical problems that increase the mortality and morbidity of our ageing society [1]. Preclinical evaluation of bone quality in animal models is currently required to determine the efficacy of novel treatments for the disease. While the ovariectomized rat model, characterized by oestrogen deficiency and accelerated bone loss, is common [2–4], the use of the ovariectomized mouse model is increasing. The mouse model is advantageous given the accessibility to inbred strains with widely varying skeletal structure and opportunities for genetic engineering [5,6]. C57BL/6 and BALB/c are two mouse strains that are examined frequently in skeletal research, e.g. for testing different anti-resorptive [7,8] or bone anabolic agents [7,9] as well as the effect of mechanical loading [9,10].

Numerous studies examining the effect of ovariectomy (OVX) have

* Corresponding author at: Department of Oncology and Metabolism, Insigneo Institute for in silico Medicine, University of Sheffield, Sheffield, UK.
E-mail address: e.dallara@sheffield.ac.uk (E. Dall'Ara).
[1] These authors contributed equally to this work.

https://doi.org/10.1016/j.bone.2019.06.024
Received 14 February 2019; Received in revised form 24 June 2019; Accepted 24 June 2019
Available online 26 June 2019

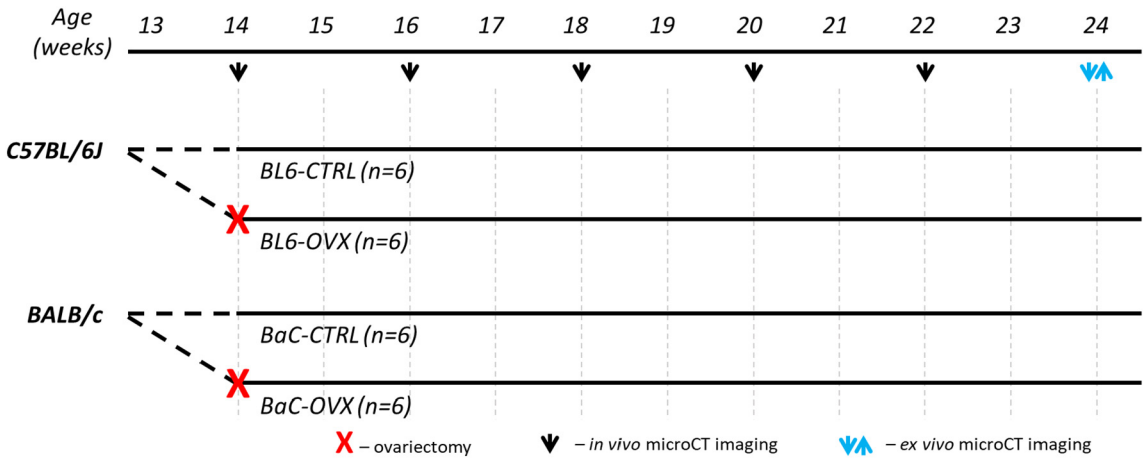

Fig. 1. Overview of study design and data collection timeline. CTRL: non-operated controls, OVX: ovariectomy. BL6: C57BL/6, BaC: BALB/c. Three mice, one each from the BL6-OVX, BaC-OVX and BaC-CTRL groups, were euthanized due to complications prior to the end of the study.

evaluated bone properties using ex vivo micro-computed tomography (microCT) [5,11], histomorphometry [12,13] and mechanical testing [13,14], performed in cross-sectional experiments where different groups of mice are compared at different time points. However, in vivo microCT imaging [15,16] combined with image registration is recommended for improving the accuracy of the measurements [17,18], which can be obtained by reducing the intrinsic variability of the animals using baseline measurements as control. Moreover, this approach allows performing dynamic morphometry, detailed densitometric evaluation and, when combined with micro-finite element (μFE) analysis, mechanical characterization [19,20] of the bone properties. Considering the reduction of variability in the measurement, this approach can reduce the number of animals used in research in line with the 3Rs (reduction, refinement and replacement of the usage of animals in research) [21].

The effect of OVX has been examined in vivo, with findings for significant intervention effects (e.g., bone loss) being dependent on the mouse strain, bone compartment (trabecular or cortical), and on time from surgery. However, some studies examined only relatively short-term (5-week post-operative) bone changes, quantifying the bone response across only 2 or 3 bone remodelling cycles [17,22]; in longer term studies (8–12 weeks) analyses were limited to a single mouse strain (C57BL/6) [19,23]; in most cases 3D bone morphometry was measured only in small regions of interest (e.g. in the metaphysis of long bones, or cortical midshaft) [17,22]; or analysed only densitometric changes in the cortical bone [23]. Also, scanning protocols in these studies [23,24] exceeded the recommendations for critical nominal ionising radiation that could affect the morphometric properties of bone [25]. Furthermore, only two studies have examined longitudinal changes in the mechanical properties of the tibiae [23] or vertebrae [19], and only from C57BL/6 subjected to OVX.

A thorough assessment of any prospective animal model of OP is recommended before the substantial investment of resources into an interventional study [26] and it is desirable that the animal model exhibits cardinal features of the human disease. OP is characterized by persistent peri- and post-menopausal bone loss [27,28] and associated with increased fragility across skeletal sites [29], which supports the need to analyse both the bone structural and mechanical properties. Moreover, as anti-osteoporotic interventions can have localized effects, e.g. as shown for teriparatide [20] and mechanical loading [10] in ovary-intact mice, an analysis across the bone length is recommended. However, to the authors' knowledge, no study in the literature has shown a comprehensive assessment of long-term changes in multiple bone properties in the murine tibia, along the tibia length and across different mouse strains. Thus, the aim of this study was to evaluate the effect of OVX on the morphometric, densitometric and estimates of mechanical properties of the tibia in two mouse strains, C57BL/6 and BALB/c. The comprehensive assessment of ovariectomy on bone properties could be useful to identify an appropriate strain for future evaluation of anti-osteoporotic treatments in the mouse model.

2. Material and methods

2.1. Animals and treatment

Twelve 13-weeks-old C57BL/6 (BL6) and twelve 13-weeks-old BALB/c (BaC) female virgin mice were purchased from Envigo RMS Ltd. (Bicester, UK). They were housed in the University of Sheffield's Biological Services Unit with a twelve-hour light/dark cycle at 22 °C and free access to food and water. All the procedures were performed under a British Home Office project licence (PPL 40/3499) and in compliance with the UK Animals (Scientific Procedures) Act 1986. This study was reviewed and approved by the local Research Ethics Committee of the University of Sheffield (Sheffield, UK). At 14-weeks old, six mice per strain underwent ovariectomy (OVX) surgery ("BL6-OVX" and "BaC-OVX" groups); the remaining mice providing non-operated controls ("BL6-CTRL" and "BaC-CTRL" groups). Success of OVX was confirmed at autopsy by weighing of the uterus. A non-operated control group was used as no systemic measurements were compared between OVX and CTRL mice and, therefore, sham surgery was not performed in order to refine the animal procedures in accordance to the 3Rs and reduce the risk of post-operative complications. Trabecular bone loss and peak cortical bone mass were documented in the appendicular skeleton of female C57BL/6 at 3–4 months old mice [30]. Thus, the mice herein were considered skeletally mature at the time of the first microCT scan (14 weeks old).

2.2. In-vivo microCT imaging

The whole right tibia of each mouse was imaged in vivo with microCT (VivaCT80, Scanco Medical, Bruettisellen, Switzerland). A baseline scan (before surgery for OVX mice) was performed at 14 weeks of age, then follow up in vivo scans were performed every two weeks until week 22 (Fig. 1). At week 24 mice were euthanized and both the left and right tibiae were imaged using the in vivo imaging protocol. Scanning parameters, optimised in a previous study [31], were: 10.4-μm isotropic voxel size, voltage of 55 kV, intensity of 145 μA, field of view of 32 mm, 1500/750 samples/projections, integration time 100 ms. This scanning protocol offered the best compromise between image quality and scanning time [31], which affect both the ionising radiation and the time in which the animal is under anaesthesia. This scanning protocol induced 256 mGy dose to the mouse, much lower

than the 434 mGy dose recommended by Laperre et al. [25] and was found to have no effect on the bone properties evaluated in this study – as determined by comparing the irradiated right tibia to the non-irradiated left tibia (Supplementary Materials Table S1). A third-order polynomial beam hardening correction algorithm based on a 1200 mg HA/cm^3 wedge phantom was applied to all the scans. A calibration law based on weekly quality checks performed on a five-rod densitometric phantom was used to convert the Hounsfield Units in each image into BMD equivalent values.

2.3. Image preprocessing

From each image three analyses were performed: standard 3D morphometric analysis, spatial densitometric analysis and estimation of the mechanical properties with μFE models. The reconstructed image of one tibia for each strain at week 14 of age was randomly chosen and used as a reference. The longitudinal axis of each reference tibia was approximately aligned with the z-axis of the global reference system [32]. All remaining images (different mice and different time points) were rigidly registered to the reference images prior to the below image analyses (sections 2.4-2.6). The rigid registrations were performed by using a Quasi-Newton optimizer and the Normalized Mutual Information as the similarity measure (Amira 5.4.3, FEI Visualization Sciences Group, France). The registered grayscale image datasets were smoothed with a Gaussian filter (convolution kernel [3 3 3], standard deviation = 0.65) in order to reduce the high frequency noise and bone voxels were defined using a global threshold, which was calculated as the average of the grey levels corresponding to the bone and background peaks in each image histogram [31].

2.4. Standard 3D morphometric analysis

For trabecular bone analysis a region of 1 mm height was selected, 0.3 mm below a reference line defined as the most distal image slice that included the growth plate and adapted from a previous study [32,33]. This was necessary in order to avoid including primary spongiosa in the region of interest (ROI). For cortical bone analysis a region of 1 mm height was selected in the tibia diaphysis and centred at 50% of the tibia bone length [32]. ROIs in the trabecular and cortical bone were manually marked and the following 3D bone parameters were computed (CT Analyser v1.18.4.0, Skyscan-Bruker, Kontich, Belgium). For trabecular bone the following parameters were evaluated: trabecular bone volume fraction (BV/TV), thickness (Tb.Th), separation (Tb.Sp) and number (Tb.N). For cortical bone the following parameters were evaluated: total cross-sectional area (Tt.Ar), cortical bone area (Ct.Ar), cortical area fraction (Ct.Ar/Tt.Ar) and cortical thickness (Ct.Th). Tibia length was computed as the distance between the most proximal and distal bone voxels in the registered image stack.

2.5. Spatiotemporal densitometric analysis

Densitometric properties were estimated in multiple regions within the tibia adapting a previously described procedure [20]. Briefly, the length of each tibia (L) was measured at each time point and a region 80% of L, and excluding the fibula, was cropped starting from the section below the growth plate (MatLab, 2015a, The MathWorks, Inc. USA). The tibia was divided longitudinally into ten transverse sections with the same thicknesses and each section was then divided into quadrants (anterior, medial, posterior and lateral sectors) for a total of 40 ROIs across the length of the tibia. Anterior, medial, posterior and lateral compartments were defined by two perpendicular lines passing through the centre of mass of each slice. Bone mineral content (BMC) and tissue mineral density (TMD) were measured in each of the 40 quadrants and in the ten sections. This approach is reproducible and accounts for small but still present growth of the tibia between weeks 14 and 24 of age [32].

TMD in each voxel was obtained from its grey level by using the calibration curve provided by the manufacturer of the microCT scanner. Each voxel BMC was calculated as TMD multiplied by the volume of the voxel. The BMC in each compartment was calculated as the sum of BMC in each bone voxel, while TMD in each compartment is defined as TMD = BMC/BV [34].

2.6. Micro-finite element models

Subject-specific μFE models of each tibia at each time point were generated [31,35]. Briefly, a connectivity filter was used to remove from the binary image the unconnected bone islands and the bone voxels were converted into 8-node hexahedral elements [36]. Bone was considered homogenous, isotropic, and linear elastic, with a modulus of elasticity of 14.8GPa, and Poisson's ratio of 0.3 [37]. Uniaxial compression was applied by fixing the nodes of the most proximal section of the model and by applying an axial displacement equal to 1 mm at the distal end. The structural apparent stiffness was calculated by μFE analysis as the measured reaction force in the longitudinal direction divided by the applied displacement. The failure load was estimated from the linear μFE models as the amount of force required for 2% of the nodes to reach the yield strain (first principal strain above 8000 microstrain or third principal strain below −10,300 microstrain [38]). The 10% of the total length was excluded from this analysis at each extremity of the model in order to reduce the boundary effects. These models have been recently validated against state-of-the-art experiments for the prediction of local deformation and structural properties, across young (16 weeks old), aged (24 weeks old) and ovariectomized (22 weeks old) female C57BL/6 mice. Absolute errors were 14% and 9% for stiffness and strength predictions, respectively [35]. The resulting linear μFE models were solved (Ansys, Release 15.0, ANSYS, Inc.) on a high-performance computing (HPC) system (Beagle, INSIGNEO, University of Sheffield; 64 cores, memory = 128GB) in approximately 70 min (5 h CPU time).

2.7. Statistical analysis

Student's *t*-tests were used to evaluate differences between CTRL and OVX mice, in bone properties at week 14, and in uterine weights at week 24. Differences between the OVX and CTRL mice (intervention effects) and between time points in each intervention group (time effect), for the 3D morphometric and densitometric (regional and total BMC) parameters, and for FE predicted stiffness and failure load, were analysed using two-way mixed Analysis of Variance (ANOVA). Where for a given parameter *F* values were significant for a “time by intervention interaction”, the simple “time effect” was investigated using paired *t*-tests between (1) baseline and proceeding time-points (weeks 16–24) and (2) between sequential time-points (e.g. week 16–18, 18–20 comparisons) [2,4]. An “intervention effect” was investigated using one-way Analysis of Covariance (ANCOVA, with adjustment for baseline values). All analyses were performed in SPSS Statistics 25 (IBM Corp., Armonk, NY). Data are presented as mean ± standard deviation (SD) unless otherwise specified. Significance level was set to $\alpha = 0.05$.

BMC and TMD values in the 10 sections and 40 ROIs across the length of the tibia are reported as the mean relative percentage difference between the ovariectomized (BL6-OVX and BaC-OVX) and intact (BL6-CTRL and BaC-CTRL) groups for each strain [20]. First for each week (j), in each compartment, the mean changes in BMC relative to the week 14 values for the CTRL ($\Delta CTRL_j$) and OVX (ΔOVX_j) groups were calculated as below:

$$\Delta \boldsymbol{CTRL_j} = \frac{\sum_{i=1}^{n1} (BMC1_{i,j} - BMC1_{i,14})}{n1}$$

$$\Delta \boldsymbol{OVX_j} = \frac{\sum_{i=1}^{n1} (BMC2_{i,j} - BMC2_{i,14})}{n1}$$

where, *n1* and *n2* are the numbers of mice in CTRL (BMC1) and OVX (BMC2) groups; *j* represents the week index and *i* represents the mouse number index.

Then for each week, in each compartment, the difference between the control ($\Delta CTRL_j$) and OVX (ΔOVX_j) groups normalized to the average BMC of the CTRL mice at that week was calculated, in order to assess the effect of ovariectomy relative to the control group. This was defined as the mean relative percentage difference ($\delta D\%_j$) and was calculated as follows:

$$\boldsymbol{\delta D\%_j} = (\Delta OVX_j - \Delta CTRL_j)/REF_j \times 100$$

where,

$$\boldsymbol{REF_j} = \frac{\sum_{i=1}^{n1} BMC1_{i,j}}{n1}$$

Similarly, mean relative percentage differences in TMD were computed as for BMC above.

3. Results

One mouse each from the BL6-OVX, BaC-OVX and BaC-CTRL groups were euthanized due to complications prior to the end of the study and thus were not included in statistical analyses. Ongoing monitoring revealed no further post-surgical complications in remaining mice, including no mobility issues when comparing OVX with non-operated CTRL and that could affect the bone properties. Bone properties did not significantly differ ($p > 0.05$) between the CTRL and OVX groups at study baseline (week 14; Tables 1,2). Uterine mass at the end of the study was significantly lower in the OVX than in the CTRL mice (in BL6, 8.6 ± 2.4 mg vs. 83.5 ± 15.4 mg; in BaC, 16.5 ± 4.4 mg vs. 141.0 ± 40.0 mg; $p < 0.001$). Data collected in this study are accessible at https://doi.org/10.15131/shef.data.8313254.

3.1. Age-related effects on the trabecular and cortical bone morphometry

A statistically significant 'time by intervention' interaction was observed, and simple time effects investigated in each mouse strain. In BL6, a detectable (statistically significant) reduction in BV/TV from baseline was observed by week 18 in OVX, and week 22 in CTRL. In BaC, significant reductions in BV/TV from baseline were observed at weeks 16 and 24 in OVX and CTRL, respectively (Table 1). In BL6-OVX, significant reductions in BV/TV were observed from week 18 until week 24; whereas in BaC-OVX, a significant reduction in BV/TV was observed only at week 16. Time-effects for remaining trabecular parameters are reported in Table 1.

A significant increase in Ct.Th was observed at week 16 in BL6-CTRL, but not until week 20 in BL6-OVX. In both BaC-CTRL and BaC-OVX, Ct.Th was significantly higher than baseline by week 20 and significantly increased thereafter until week 24. Time-effects for remaining cortical parameters are reported in Table 2.

3.2. Effects of OVX on tibia length and trabecular and cortical bone morphometry

Tibia length, adjusted for week 14 values, was significantly higher from week 16 in both BL6 and BaC ($p < 0.01$, Fig. 2). At week 24, tibia length had increased from week 14 baseline between 4.1 and 4.5% for the OVX groups and between 3.0 and 3.2% for the CTRL groups (equivalent to a mean change of 0.51 to 0.55 mm and 0.72 to 0.79 mm, respectively).

Tibia trabecular bone morphometry (group means, adjusted for week 14 baseline) also differed with OVX (Table 1, Figs. 3, 4). BV/TV was significantly lower in BL6-OVX than BL6-CTRL from week 18 onward (peak 38% lower at week 22, Table 1) and attributed to 10–22% lower Tb.N (from week 18 to week 24) and 25–37% higher Tb.Sp (from week 20 to week 24). Tb.Th was significantly lower at weeks 16 to 20, but did not significantly differ thereafter. In BaC-OVX, BV/TV and Tb.N were significantly lower than BaC-CTRL, only at weeks 16 to 20 (BV/TV: 11–25% lower; Tb.N: 8–19% lower), and Tb.Sp significantly higher from week 16 to 24 (up to +45%).

In BL6-OVX, the cortical midshaft was significantly thinner (relative increase in Ct.Th was 3.7–5.3% lower in OVX than CTRL) and the Ct.Ar/Tt.Ar was significantly lower (relative increase 3.3–4.5% lower) than in BL6-CTRL from week 16 to week 24 (Fig. 3, Table 2). Cortical bone morphometry did not differ significantly between BaC-CTRL and BaC-OVX. Individual trends for both trabecular and cortical bone morphometry are reported in the Supplementary Materials.

3.3. Effects of OVX on the tibia bone densitometric properties

For BMC, OVX-effects were observed in each section (sum of BMC in the four quadrants per section) and in each quadrant (regional BMC, Fig. 5) for both mouse strains. BMC and TMD increased over time in all ten sections in both OVX and CTRL (data not shown). For BL6, the relative percentage difference in BMC in the proximal tibia (C01) was significant and negative from week 16 onward (increasing from −4% at week 16 to −18% at week 24, all $p < 0.05$, Fig. 5). A negative change indicates a smaller increase in BMC, normalized for baseline, in the OVX than in CTRL mice. At week 24, the percentage difference was negative in remaining cross-sections (−4% to −8% vs. CTRL in C02–04, C09). In BaC, the percentage difference was significant and negative in C01 and at weeks 18, 22 and 24 (−11% to −12%, all $p < 0.05$; Fig. 5). A positive percentage difference in BMC (indicating a greater increase of BMC in OVX than CTRL) was observed in the mid- and distal diaphysis (in C05-C06, +4% to +5% at weeks 20, 22; in C08-C09, +4% to +9% higher at weeks 18–24).

Statistically significant differences in BMC, between OVX and CTRL, were observed in all quadrants after week 18 (Supplementary Materials). In BL6, the percentage difference medially was negative, whereas laterally a positive percentage difference was observed (Fig. S3). Consequently, the percentage differences for BMC summed over each section (as reported in Fig. 5) were small and non-significant. In BaC, differences in the four quadrants (medial, lateral, anterior, posterior) were consistent with spatiotemporal patterns of change in the BMC summed over the sections.

For TMD, negative percentage differences (indicating a smaller increase in TMD in OVX than CTRL) were observed in both BL6 and BaC (Fig. 6). In BL6, the percentage differences were significant in C01 at weeks 18–20 (−4%) and in C01–C02 at week 24 (−3% to −4% vs. CTRL). In BaC-OVX, significant differences were observed in C01 at weeks 20–24 (−3% to −5% vs. CTRL). Regionally, small differences were evident in the proximal sections of the tibia (Fig. S4).

3.4. Effects of OVX on the tibia bone mechanical properties

OVX had no effect on μFE estimates of bone stiffness or failure load in neither strain of mouse (Fig. 7). Nor were age-related changes evident in either mechanical property of the tibia bone in mice with or without ovariectomy.

4. Discussion

In this study, a comprehensive assessment on the effect of ovariectomy on the morphometric, densitometric and μFE estimates of mechanical properties of the tibia in two strains of mice was performed. The results herein suggest a strain-, region- (trabecular or cortical) and time-dependent response of the bone properties to oestrogen-deficiency in these mouse models of osteoporosis. This data extends upon previous longitudinal research on the murine tibia, examining intervention effects to 10 weeks following ovariectomy and that was quantified previously until only 5 weeks following surgery [22]. Further, we

Table 1
Tibial metaphyseal trabecular 3D bone morphometry in two strains of mouse with and without ovariectomy (values reported as mean ± standard deviation).

		Age (weeks)					
		14+	16	18	20	22	24
C57BL/6							
BV/TV (%)	CTRL	6.75 ± 1.13	6.53 ± 0.79	6.00 ± 0.80	5.72 ± 0.99	5.28 ± 0.91	4.50 ± 0.85
	OVX	6.27 ± 1.19	5.56 ± 1.18	4.26 ± 0.91	3.11 ± 0.43	2.92 ± 0.53	2.49 ± 0.30
	% difference		-7.2	-18.6**	-27.8**	-37.8**	-22.7**
	Time-effect:		(0.544)	(0.215;0.202)	(0.099;0.263)	(**0.021;0.011**)	(**0.005;0.002**)
	CTRL		(0.186)	(**0.027;0.007**)	(**0.001;0.019**)	(**0.001**;0.083)	(**0.001;0.033**)
	OVX						
Tb.Th (μm)	CTRL	45 ± 5	47 ± 5	49 ± 4	52 ± 4	52 ± 5	52 ± 4
	OVX	45 ± 3	42 ± 2	44 ± 3	46 ± 3	48 ± 6	49 ± 6
	% difference		-9.2*	-9.7**	-10.7**	-6.3	-5.3
	Time-effect:		(0.055)	(**0.027**;0.129)	(**0.003**;0.071)	(**0.006**;0.911)	(**0.004**;0.169)
	CTRL		(0.125)	(0.753,0.221)	(0.210,0.167)	(0.063,0.148)	(0.064,0.155)
	OVX						
Tb.Sp (μm)	CTRL	325 ± 58	342 ± 61	362 ± 62	364 ± 55	388 ± 78	409 ± 70
	OVX	331 ± 29	390 ± 35	411 ± 64	450 ± 75	483 ± 73	535 ± 86
	% difference		12.9	13.0	24.8*	27.5*	37.1**
	Time-effect:		(0.137)	(0.060;0.313)	(**0.037**;0.921)	(**0.007**;0.193)	(**0.004**;0.084)
	CTRL		(**0.048**)	(0.078;0.485)	(**0.033;0.014**)	(**0.013;0.015**)	(**0.007;0.006**)
	OVX						
Tb.N (1/mm)	CTRL	1.50 ± 0.32	1.39 ± 0.18	1.23 ± 0.23	1.12 ± 0.23	1.04 ± 0.25	0.87 ± 0.23
	OVX	1.40 ± 0.19	1.31 ± 0.25	0.98 ± 0.23	0.68 ± 0.11	0.61 ± 0.10	0.51 ± 0.08
	% difference		1.9	-9.7**	-22.0**	-21.2**	-16.9**
	Time-effect:		(0.143)	(**0.029;0.036**)	(**0.014;0.017**)	(**0.004;0.030**)	(**0.001; < 0.001**)
	CTRL		(0.326)	(**0.018;0.002**)	(< **0.001;0.010**)	(< **0.001;0.003**)	(< **0.001;0.008**)
	OVX						
BALB/c							
BV/TV (%)	CTRL	9.69 ± 1.20	9.38 ± 1.78	8.90 ± 1.29	7.87 ± 0.97	7.44 ± 0.95	6.44 ± 0.65
	OVX	8.73 ± 1.16	6.04 ± 0.68	5.68 ± 0.94	5.89 ± 1.31	6.10 ± 2.08	5.87 ± 2.03
	% difference		-24.6**	-23.3**	-10.6*	-4.0	4.0
	Time-effect:		(0.643)	(0.225;0.146)	(**0.022;0.003**)	(**0.026**;0.078)	(**0.004;0.003**)
	CTRL		(**0.003**)	(< **0.001**;0.477)	(< **0.001**;0.422)	(**0.011**;0.613)	(**0.011**;0.416)
	OVX						
Tb.Th (μm)	CTRL	47 ± 1	48 ± 4	51 ± 3	51 ± 2	52 ± 2	51 ± 3
	OVX	46 ± 2	45 ± 3	48 ± 3	50 ± 5	51 ± 6	51 ± 6
	% difference		-6.5	-5.8	-2.0	-2.1	0.2
	Time-effect:		(0.265)	(**0.002;0.043**)	(**0.002**;0.352)	(**0.001**;0.101)	(**0.009**;0.249)
	CTRL		(0.422)	(0.167;0.106)	(0.120;0.182)	(0.077;0.132)	(0.100;0.990)
	OVX						
Tb.Sp (μm)	CTRL	257 ± 30	276 ± 24	292 ± 20	323 ± 27	348 ± 32	371 ± 27
	OVX	287 ± 23	383 ± 25	437 ± 33	441 ± 31	459 ± 36	469 ± 26
	% difference		30.0**	44.8**	34.3**	31.7**	26.5**
	Time-effect:		(**0.003**)	(**0.005;0.024**)	(**0.001;0.005**)	(< **0.001;0.011**)	(< **0.001;0.027**)
	CTRL		(**0.001**)	(**0.001;0.042**)	(< **0.001**;0.836)	(**0.001**;0.096)	(< **0.001**;0.507)
	OVX						
Tb.N (1/mm)	CTRL	2.08 ± 0.23	1.94 ± 0.24	1.73 ± 0.22	1.55 ± 0.18	1.42 ± 0.15	1.26 ± 0.10
	OVX	1.87 ± 0.17	1.34 ± 0.10	1.17 ± 0.14	1.17 ± 0.15	1.17 ± 0.25	1.13 ± 0.23
	% difference		-18.9**	-17.4**	-8.3**	-2.3	3.5
	Time-effect:		(0.187)	(**0.042;0.019**)	(**0.007;0.001**)	(**0.008**;0.050)	(**0.001;0.009**)
	CTRL		(< **0.001**)	(< **0.001**;0.053)	(< **0.001**;0.888)	(**0.001**;0.933)	(< **0.001**;0.335)
	OVX						

BV/TV: trabecular bone volume fraction, Tb.Th: trabecular thickness, Tb.Sp: trabecular separation, Tb.N: trabecular number. % difference determined as the mean percentage difference of the change of each parameter (change relative to baseline) between control (CTRL) and ovariectomized (OVX) groups, normalized by CTRL. See section 2.7 in the manuscript for computation.

* $p < 0.05$.

** $p < 0.01$ indicates statistically significant differences in bone parameter between CTRL and OVX. P-values for a time-effect are reported in parentheses as (comparison to baseline values;comparison previous time point). P Values in bold indicate a statistically significant difference between time points. +Morphometric properties did not differ between the CTRL and OVX mice at week 14 baseline (Student's t-test).

quantified OVX-effects on multiple bone properties in two common mouse strains and with an imaging protocol that has minimal radiation effects on the observed measures. Changes in the three bone properties were quantified in the same BL6 mice, which were computed among separate studies previously [22,23] and densitometric and mechanical changes were determined in BaC for the first time.

We observed a significant OVX-effect for increased tibia length in both mouse strains, consistent with cross-sectional observations in juvenile (4–8 weeks old) ovariectomized mice [39,40]. Similarly, Lu et al. [23] report a greater, albeit non-statistically significant, increase in the tibia length of OVX than sham operated BL6 mice from 14 to 22 weeks old (3.7% vs. 2.5% increases in tibia length, respectively). In developing mammals, oestrogen is vital for the cessation of linear growth and growth plate closure at sexual maturity. However, in rodents the growth plate does not close and ovariectomy and associated oestrogen-deficiency promotes continued longitudinal bone growth, in part, through an increase in chondroblasts in the proliferative zone of the growth plate [41]. In human OP, oestrogen-deficiency affects changes in bone width but not in length, given that epiphyseal closure occurs many decades before the onset of menopause [42]. Herein, a slowing of the tibia growth rate was observed by week 24 and documented elsewhere up to 12 months old [43]. However, we selected younger mice to

Table 2
Tibial cortical midshaft 3D bone morphometry in two strains of mouse with and without ovariectomy (values reported as mean ± standard deviation).

		Age (weeks)					
		14+	16	18	20	22	24
C57BL/6							
Tt.Ar (mm^2)	CTRL	0.83 ± 0.05	0.86 ± 0.04	0.87 ± 0.04	0.88 ± 0.05	0.89 ± 0.04	0.88 ± 0.04
	OVX	0.84 ± 0.04	0.88 ± 0.03	0.89 ± 0.02	0.90 ± 0.03	0.90 ± 0.04	0.90 ± 0.04
	% difference		0.6	1.2	1.2	0.2	0.4
	Time-effect:		(< **0.001**)	**(< 0.001;0.036)**	(< **0.001**;0.180)	**(< 0.001;0.026)**	(**0.002**;0.692)
	CTRL		(**0.007**)	(**0.030**;0.233)	(**0.031**;0.185)	(**0.030**;0.597)	(**0.030**;0.928)
	OVX						
Ct.Ar (mm^2)	CTRL	0.48 ± 0.05	0.51 ± 0.05	0.52 ± 0.05	0.53 ± 0.05	0.54 ± 0.04	0.53 ± 0.04
	OVX	0.50 ± 0.03	0.51 ± 0.03	0.52 ± 0.02	0.53 ± 0.02	0.54 ± 0.02	0.53 ± 0.02
	% difference		-1.6	-3.4	-2.6	-3.1	-3.7**
	Time-effect:		**(0.003)**	**(0.001;0.001)**	**(0.002;0.004)**	**(0.001;0.038)**	(**0.003**;0.350)
	CTRL		**(0.012)**	(**0.008**;0.376)	**(0.005;0.026)**	(**0.005**;**0.026**)	(**0.006**;0.059)
	OVX						
Ct.Ar/Tt.Ar (%)	CTRL	57 ± 3	59 ± 3	60 ± 3	60 ± 3	60 ± 2	60 ± 2
	OVX	59 ± 1	59 ± 1	59 ± 1	59 ± 1	60 ± 1	59 ± 1
	% difference		-2.3	-4.5*	-3.8*	-3.3**	-4.0**
	Time-effect:		(**0.014**)	(**0.001;0.001**)	(**0.003**;0.139)	(**0.003**;0.778)	(**0.003**;0.943)
	CTRL		(0.652)	(0.874,0.893)	(0.350,0.074)	(0.206,0.138)	(0.511,**0.038**)
	OVX						
Ct.Th (μm)	CTRL	196 ± 16	203 ± 16	210 ± 16	212 ± 15	213 ± 13	212 ± 12
	OVX	201 ± 6	205 ± 9	206 ± 8	209 ± 7	211 ± 7	208 ± 8
	% difference		-1.7	-5.3	-4.2*	-3.7**	-5.0**
	Time-effect:		(**0.004**)	(**0.001; < 0.000**)	(< **0.000**;0.108)	(**0.001**;0.433)	(**0.001**;0.705)
	CTRL		(0.096)	(0.159,0.984)	(**0.023,0.030**)	(**0.021**,0.070)	(0.066,**0.008**)
	OVX						
BALB/c							
Tt.Ar (mm^2)	CTRL	0.77 ± 0.04	0.77 ± 0.04	0.78 ± 0.05	0.78 ± 0.05	0.79 ± 0.05	0.80 ± 0.05
	OVX	0.81 ± 0.04	0.81 ± 0.04	0.80 ± 0.04	0.82 ± 0.04	0.82 ± 0.04	0.83 ± 0.04
	% difference		-0.2	-1.2	0.2	-0.7	-0.8
	Time-effect:		(0.604)	(0.685;0.095)	(0.469;0.281)	(0.069;**0.018**)	(**0.040**;0.119)
	CTRL		(0.271)	(0.281;0.468)	(0.161;**0.011**)	(0.226;0.623)	(0.123;0.279)
	OVX						
Ct.Ar (mm^2)	CTRL	0.54 ± 0.03	0.54 ± 0.04	0.56 ± 0.04	0.57 ± 0.04	0.58 ± 0.04	0.59 ± 0.04
	OVX	0.57 ± 0.03	0.57 ± 0.02	0.58 ± 0.02	0.60 ± 0.03	0.61 ± 0.02	0.61 ± 0.03
	% difference		-1.0	-1.0	1.3	0.2	-0.4
	Time-effect:		(0.589)	(**0.025;0.008**)	(**0.013;0.007**)	(**0.003;0.001**)	(**0.007**;0.053)
	CTRL		(0.415)	(**0.018;0.003**)	(**0.001;0.001**)	(**0.002**;0.415)	(**0.002**;0.292)
	OVX						
Tt.Ar/Ct.Ar (%)	CTRL	70 ± 1	71 ± 1	72 ± 2	73 ± 2	73 ± 2	74 ± 2
	OVX	70 ± 2	70 ± 2	72 ± 2	73 ± 2	74 ± 2	74 ± 3
	% difference		-0.8	0.1	0.8	0.6	0.1
	Time-effect:		(0.132)	(**0.003;0.007**)	(**0.002**;0.117)	(**0.001;0.033**)	(**0.004**;0.147)
	CTRL		(0.520)	(**0.002; < 0.001**)	(< **0.001;0.003**)	(< **0.001;0.038**)	(**0.001**;0.444)
	OVX						
Ct.Th (μm)	CTRL	252 ± 11	255 ± 13	263 ± 14	267 ± 12	270 ± 12	275 ± 14
	OVX	258 ± 11	259 ± 11	270 ± 8	277 ± 10	279 ± 10	282 ± 14
	% difference		-0.8	0.1	1.8	1.1	0.6
	Time-effect:		(0.229)	(**0.008;0.006**)	(**0.002;0.035**)	(**0.001;0.007**)	(**0.005;0.005**)
	CTRL		(0.376)	(**0.003;0.002**)	(< **0.001; < .001**)	(< **0.001**;0.118)	(**0.001;0.001**)
	OVX						

Tt.Ar: Total cross-sectional area, Ct.Ar: cortical bone area, Ct.Ar/Tt.Ar: cortical area fraction, Ct.Th: cortical thickness. % difference determined as the mean percentage difference of the change of each parameter (change relative to baseline) between control (CTRL) and ovariectomized (OVX) groups, normalized by CTRL. See section 2.7 in the manuscript for computation. *p < 0.05 indicates statistically significant differences in bone parameter between CTRL and OVX. P Values for a time-effect are reported in parentheses as (comparison to baseline values;comparison to previous time point). P Values in bold indicate a statistically significant difference between time points. +Morphometric properties did not differ between the CTRL and OVX mice at week 14 baseline (Student's t-test).

minimize the effects on bone of age-related comorbidities that may be considered concurrently in future research. With respect to repeated microCT scans, while larger levels of ionising radiation (between 1.65 and 17.5 Gy) were found to retard longitudinal growth in the rat tibia [44,45], our repeated scans (at 256 mGy; more than one to two orders of magnitude lower than therapeutic dose) did not affect tibia length when comparing between the irradiated and non-irradiated limbs (see Supplementary Materials Table S1).

In the standard 3D bone morphometry analyses, we confirmed age-related trabecular bone loss in the tibial metaphysis as previously reported in skeletally mature BL6 and BaC mice (~3 months of age) [22,30]. Our results also suggest a strain- and time-dependent response of the trabecular and cortical bone morphometry to OVX. In BL6 a significant OVX-related reduction in trabecular bone mass was evident after 4 weeks and persisting until 10 weeks post-operatively, in contrast with prior longitudinal research in the tibia of this mouse strain that reported no intervention effect within 5 weeks from surgery [22]. However, Klinck and Boyd [22] included, in part, the primary spongiosa in their analyses, and thus quantified morphometry of both the remodelled secondary and newly formed primary trabeculae. We minimized inclusion of the primary spongiosa by offset of the trabecular ROI analysed herein. The persistent bone loss is consistent with observations in the tibia metaphysis of ovariectomized Wistar rats, a common model for OP [2,3,46], and reflects the human disease [27].

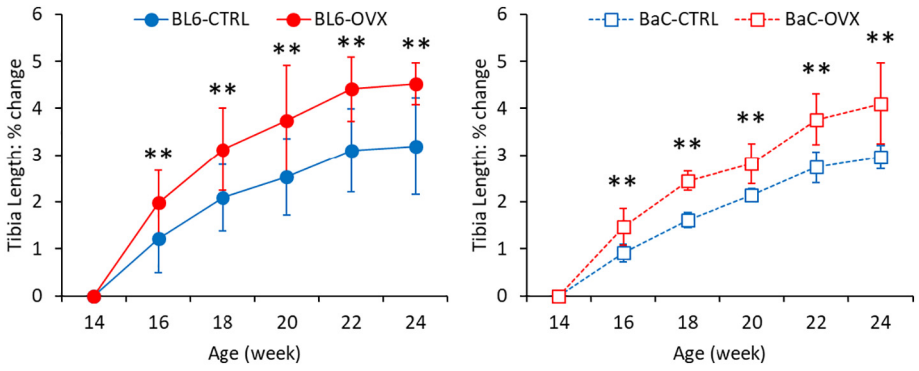

Fig. 2. Mean percentage change from 14 weeks baseline (and standard deviation (error bars)) in tibia length over time in two strains of mice, (left) C57BL/6 and (right) BALB/c, with and without ovariectomy. **p < 0.01 indicates statistically significant differences in relative change in tibia length between control (CTRL) and ovariectomized (OVX) mice (ANCOVA, adjusted for baseline values at week 14).

Meanwhile, OVX-related bone deficits, from 4 to 12 weeks post-surgery, were reported in the BL6 caudal vertebra in mice aged 14 weeks at baseline [19]. However, bone adaptation differs between the appendicular and axial skeleton [5], thus, one could not infer that long-term changes in the vertebra were likely to reflect long-term changes also in the load-bearing hind-limbs. In BaC, a significant OVX-effect was observed within 2–4 weeks from surgery but not thereafter, consistent with previous research and in support for a transient intervention effect in this strain [5,22]. Interestingly, whereas BL6 show a steady decline in BV/TV, in BaC, BV/TV decreases rapidly (BV/TV decreasing from 8.7% to 6.0% from weeks 14 to 16, Table 1) and skeletal homeostasis (a plateau in BV/TV values) was observed by week 18 despite a persistent increase in Tb.Sp in the operated group. Whether this reflects a physiological limit for bone loss, or as suggested by Klinck et al. [22] is due to greater physical activity in BaC remains unclear. A plateau in BV/TV was shown in Sprague-Dawley rats [4] and ovariectomized sheep [47]; this effect in the latter attributed to extragonadal oestrogen. Nevertheless, morphometric analysis with visual inspection of microCT scans suggests that OVX-related bone loss was due, in both strains, to trabecular thinning (early reduction in Tb.Th) and resorption of whole trabeculae (decrease in Tb.N and increase in Tb.Sp), particularly of the structures furthest from endosteal surfaces (see Fig. 4).

For midshaft cortical bone, intervention effects, characterized by lower Ct.Ar/Tt.Ar and Ct.Th, were evident only in BL6 and consistent with cross-sectional studies in the murine femoral midshaft [5,22]. The thinner cortical bone with similar cross-sectional area (Tt.Ar) suggests that OVX-related differences are due to endosteal resorption and that oestrogen deficiency does not influence periosteal expansion consistent with findings in 5–8 weeks old ovariectomized mice [48]. Nevertheless, given the small differences in mean Ct.Th between the two groups (2 to 10 μm differences between OVX and CTRL) and small change in mean Ct.Th across time-points (up to 24 μm increase in Ct.Th from week 14 to 24; see Table 2), further volumetric analyses in different regions of the tibia is recommended. Moreover, our relatively large voxel size (10 μm^3) precludes analysis of cortical porosity, which was shown to differ with OVX [13,49]. Thus, strain- and time-dependent changes in the cortical microstructure require further investigation to confirm intervention-related effects at the endosteal surface. Interestingly, our findings support the hypothesis that mice with high cortical bone volume (i.e. in BaC) may be more protected against OVX-related bone loss than mice with lower baseline properties (i.e. in BL6), though the mechanism remains unclear [5].

In both strains, a significant OVX-related reduction in the BMC was observed in the proximal tibia, where trabecular bone loss was evident and consistent with previous research [23]. Beyond resorption of trabeculae, observations at C01 may also reflect changes in bone modelling (and new bone formation) that occurs close to the growth plate and may be accelerated with oestrogen-deficiency [40]. This is supported by the smaller increase we observed in C01 TMD which could suggest recent ossification, and thus less mineralized bone, in the proximal

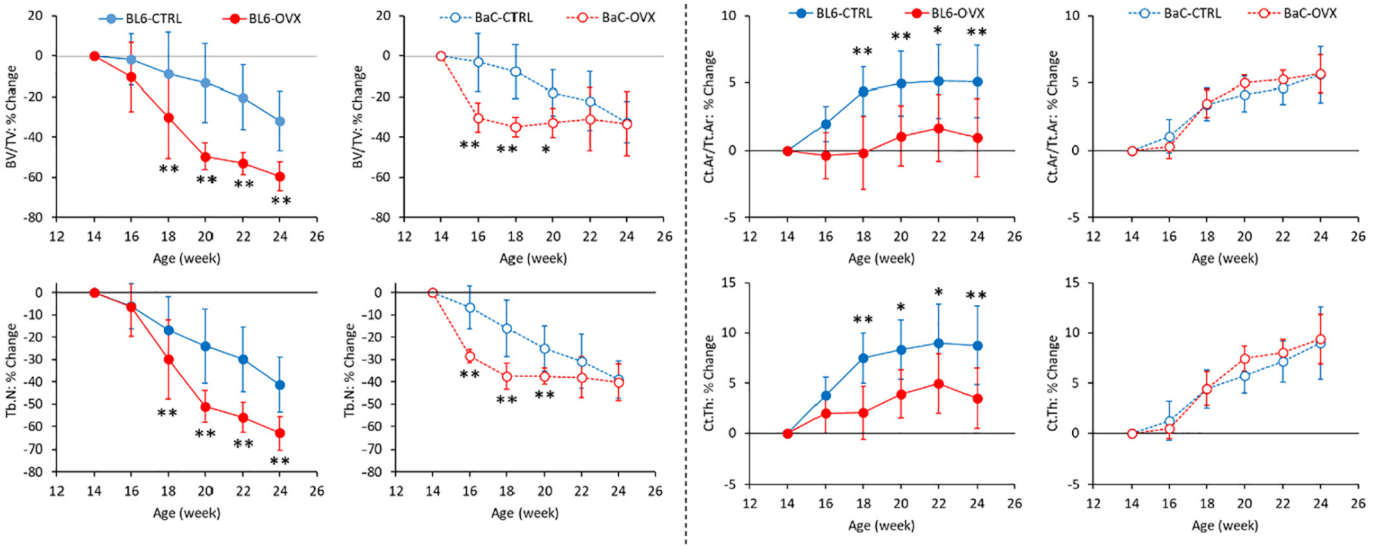

Fig. 3. Mean percent change from 14 weeks baseline (and standard deviation (error bars)) of (left) metaphyseal trabecular and (right) cortical midshaft 3D bone morphometry over time in the tibia of two strains of mouse (C57BL/6 and BALB/c) with and without ovariectomy. BV/TV: trabecular bone volume fraction; Tb.N: trabecular number; Ct.Ar/Tt.Ar: cortical area fraction; Ct.Th: cortical thickness. *p < 0.05, **p < 0.01 indicates statistically significant differences in mean bone morphometry values between control (CTRL) and ovariectomized (OVX) mice (ANCOVA, adjusted for baseline values at week 14). See supplementary materials for individual trends in each mouse.

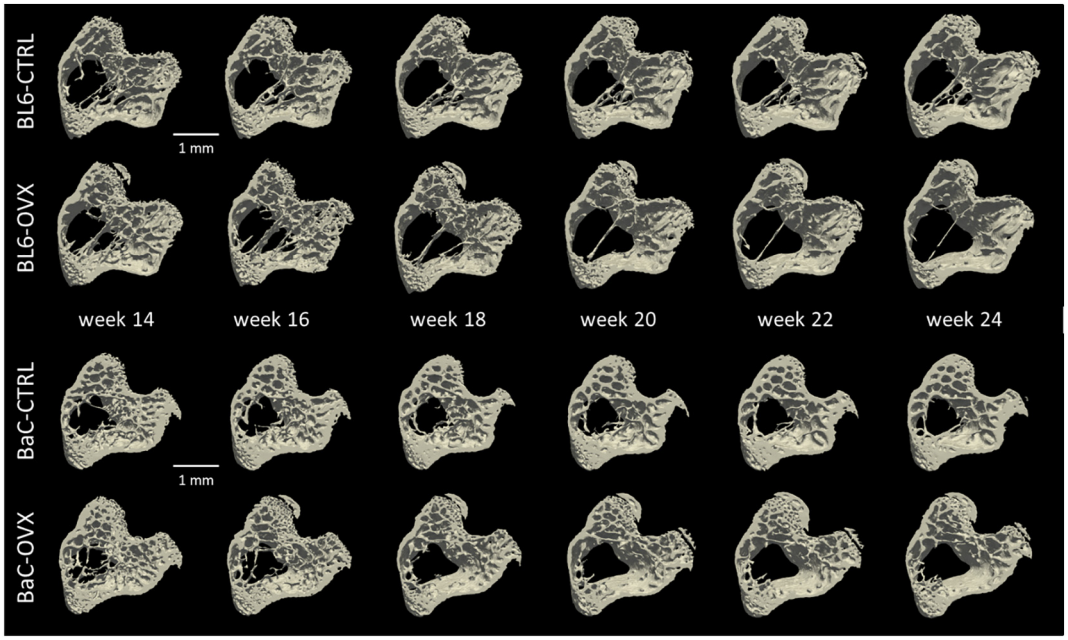

Fig. 4. Trabecular bone in the murine tibia metaphysis of representative mice from the four study groups. The figure highlights age-related (in control (CTRL)) and ovariectomy (OVX)-related bone loss in these skeletally mature C57BL/6 (BL6) and BALB/c (BaC) mice. OVX was performed at week 14.

C57BL/6

BMC [% diff]	W16	W18	W20	W22	W24
C01	-6*	-15**	-15**	-15**	-18**
C02	0	-2	-3	-5	-8**
C03	-2	-1	0	-2	-4*
C04	-1	0	-2	-4*	-6**
C05	0	1	3	1	1
C06	-2	-4	-3	-3	-3
C07	-1	0	1	2	-3
C08	-2	-1	4	0	-2
C09	-1	-2	-2	-3	-4**
C010	0	0	-6	-1	-6

BALB/c

BMC [% diff]	W16	W18	W20	W22	W24
C01	-1	-11*	-8	-11*	-12**
C02	2	2	1	-1	-3
C03	1	3	3	2	0
C04	2	2	3	3	0
C05	2	2	4**	4*	2
C06	2	1	5**	4**	2
C07	1	-2	2	2	-2
C08	3	7**	7**	9**	9**
C09	2	4*	4*	6**	5**
C010	1	-1	3	4	2

Fig. 5. Longitudinal effects of ovariectomy on the bone mineral content (BMC) in ten sections along the tibia length in (left) C57BL/6 and (right) BALB/c mice. Values are reported as the mean relative percentage difference between control and OVX mice, normalized for the baseline values of CTRL group. Refer to section 2.7 in the manuscript for computation. *p < 0.05, **p < 0.01 indicates statistically significant differences between control and ovariectomized mice (ANCOVA, adjusted for baseline values at week 14).

tibia. The higher increase in BMC at the mid- and distal diaphysis in BaC-OVX is of interest. Notably, this positive intervention effect occurs about the distal tibio-fibular junction. Thus, differences could be attributed to the small, but still present longitudinal growth of the tibia that is affected by OVX (Fig. 2), and that influences the amount of bone about the distal tibio-fibular junction that was included in analysis of these tibia cross-sections. Overall, this finding highlights a site-specific and conflicting response in BMC along the bone length following OVX. Such region-dependent discrepancies, i.e. higher or lower mineral content following OVX, were similarly observed at the trabecular-level between cross-sectional studies of the sheep and rat that examined bone in proximal femur and the tibia metaphysis, respectively [50]. Further, reductions in mineralization were not found to be uniform in the proximal femur in the ovine model of OP; this variability potentially a response to local variation in the mechanical environment [51]. Why similar effects are therefore not present in BL6 may be due to the

C57BL/6

TMD [% diff]	W16	W18	W20	W22	W24
C01	-1	-4**	-4**	-2	-4**
C02	-1	-1	-2	-2	-3*
C03	-1	-1	-1	-1	-2
C04	-1	0	-1	-1	-2
C05	-1	0	0	0	-1
C06	-1	0	0	0	-1
C07	-1	0	0	0	-1
C08	-1	0	0	0	-1
C09	0	1	0	0	-1
C010	0	1	1	1	-1

BALB/c

TMD [% diff]	W16	W18	W20	W22	W24
C01	0	-2	-3**	-4**	-5**
C02	0	-1	-1	-1	-2
C03	0	0	0	0	-1
C04	1	0	0	0	0
C05	0	0	0	0	-2
C06	0	0	0	0	0
C07	0	0	0	1	0
C08	0	0	0	1	0
C09	0	1	0	1	0
C010	0	1	0	0	0

Fig. 6. Longitudinal effects of ovariectomy on the tissue mineral density (TMD) in ten sections along the tibia in (left) C57BL/6 and (right) BALB/c mice. Values are reported as the mean relative percentage difference between control and OVX mice, normalized for the baseline values of CTRL group. Refer to section 2.7 in the manuscript for computation. *p < 0.05, **p < 0.01 indicates statistically significant differences between control and ovariectomized mice (ANCOVA, adjusted for baseline values at week 14).

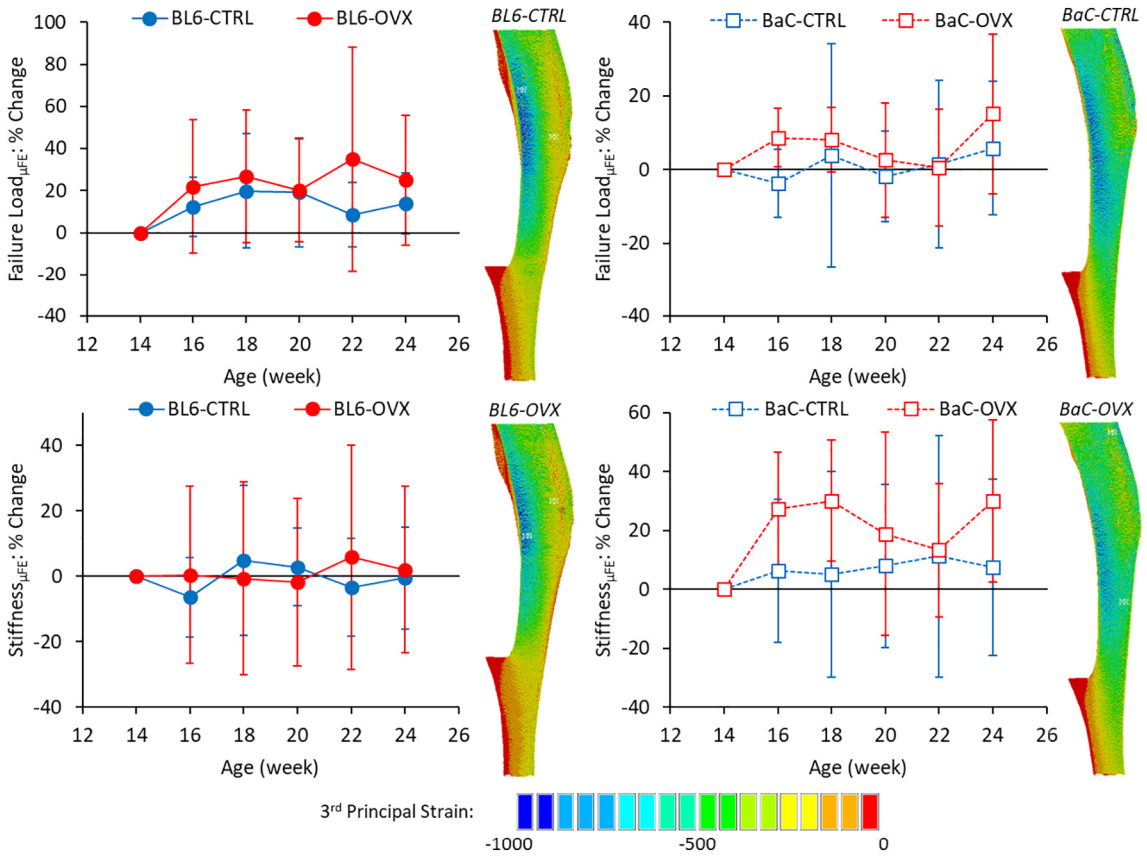

Fig. 7. Mean percent change from 14-week baseline (and standard deviation (error bars)) of μFE estimates of (top row) bone strength (failure load) and (bottom row) bone stiffness over time in the tibia of two strains of mouse (C57BL/6 and BALB/c) with and without ovariectomy. The distribution of the 3rd principal strains over the mouse tibia at week 24 are shown for a representative mouse from each strain and each intervention.

different geometry in the tibio-fibular junction between the two mice strain. Overall, the densitometric analysis provides a more comprehensive overview on heterogeneous spatiotemporal changes due to ovariectomy, as applied to multiple regions across the tibia length, than from the standard 3D morphometry alone.

Despite OVX-induced changes in morphometric and densitometric properties, no statistically significant changes in the μFE estimates of bone mechanical properties were revealed in either mouse strain and consistent with previous research [23]. However, no ageing-related changes in μFE predicted bone mechanics in CTRL nor OVX mice were observed, inconsistent with the age-related increments in tibia stiffness and strength as reported elsewhere [23]. In murine caudal vertebra, a significant OVX-related reduction in μFE estimates of bone stiffness were found and corresponding with significant reductions in trabecular and cortical bone mass [19]. This finding suggests a strong dependence of bone mechanics on bone morphometry in the axial skeleton, which is supported experimentally in murine L6 vertebra for failure load [52]. Nevertheless, under compression the trabecular bone in the mouse tibia has a minimal impact on the bone stiffness and strength as reported in the preliminary data shown by Oliviero et al. [31]. Therefore, changes in the morphometric properties of trabecular bone are not expected to reflect changes in tibia stiffness and strength under compressive load, and the small changes in cortical bone observed for BL6 mice at week 24 of age may be too small to affect the mechanical properties of the tibia in uniaxial compression. Nevertheless, we do not exclude that invasive micromechanical testing and/or nanoindentation would reveal OVX-related differences in bone mechanics as shown previously [13,14,50]. However, the destructive nature of such tests prohibit a longitudinal study design, thus we selected μFE modelling, in a simple loading configuration and validated previously [35], for investigating age- and OVX-related changes in bone biomechanics.

The data herein, from two mouse models of human OP, may highlight different aspects of the disease. OP is characterized by the rapid peri- and persistent post-menopausal reductions in bone mass. Thus, the use of BaC and BL6, which are common strains for preclinical assessment of anti-osteoporotic therapies, may be most appropriate to study short (2–4 week) and long-term (4+ week) treatment effects, respectively. Moreover, this data highlights the importance of study length, selection of anatomical locations and use of multiple structural properties for understanding the effects of oestrogen deficiency and that may help explain discrepancies among previous studies. Given the heterogeneous time- and region-dependent response of the bone following OVX and to anti-osteoporotic therapies [10,20], and strong structure-mechanics relationships of bone documented elsewhere [50], we recommend measurement of the bone morphometric, densitometric and mechanical properties in such longitudinal studies; these measures that can be computed from repeated scans of the whole mouse tibia.

4.1. Limitations

There were several limitations in our study. First, the in vivo study design precludes microCT scanning with smaller voxel size without increasing the radiation dose. Thus, we could not directly evaluate the effects of OVX on intra-cortical bone resorption observed previously in oestrogen-deficient mice [13,49]. Nevertheless, while a larger voxel size is known to overestimate the thickness of trabeculae (e.g. +15% higher Tb.Th at 10 μm than 5 μm in the mouse tibia metaphysis [31]), 10 μm, which is approximately one-fourth to one-fifth the mean trabecular thickness, is within guidelines to resolve the mouse trabecular bone [15] and consistent with, or smaller than, voxel size reported in previous longitudinal studies of the ovariectomized mouse [17,19,22,23]. Second, microCT scans were performed at 2-week

intervals and thus intermediate bone adaptations could not be quantified during the murine bone turnover cycle (~2 weeks length [6]). However, the loss of spatial and temporal resolution was necessary for minimising radiation dose (total and per scanning session), to mitigate the significant effects of ionising radiation on bone morphometry and to enable the longitudinal study design in which we quantify OVX changes to 10 weeks. Third, we had a modest sample size (n = 5–6 mice/group), which given the heterogeneous response of the mice following OVX (e.g. a transient response of trabecular bone in a BaC mouse (see Supplementary Materials)) may confound group trends and limit our ability to detect significant intervention effects. However, the longitudinal design with appropriate statistical methods (ANCOVA with adjustment for baseline values to investigate intervention effects) is advantageous, to reduce risk of study bias while improving study power. A fourth limitation was the use of simple (but efficient) homogeneous isotropic linear voxel-based μFE models, although recently we show that these predict well, with 9–14% absolute errors against experimental measurements, the murine tibia stiffness, strength and local displacements across young, older and ovariectomized BL6 mice [35]. Whether these errors would affect the OVX and intact groups of BaC mice equally is uncertain. Thus, we caution in the interpretation of findings given that the suitability of the μFE approach to distinguish among groups in this strain is still to be explored. Nevertheless, work is ongoing for optimising the μFE modelling protocol, including implementing heterogeneous material properties based on local mineralization and improving boundary recovery by tetrahedral meshing. Finally, the standard morphometric analysis does not account for both longitudinal growth and the formation of new bone at the growth plate. Thus, with time from baseline the trabeculae examined will include a combination of both the newly formed and remodelled bone, which requires more deliberate methods to separate these processes that may be affected by ageing and OVX differently. For example, dynamic 3D bone morphometry to study local effects of *bone remodelling*, as has been described elsewhere [19,53] and that was beyond the scope of this paper.

4.2. Conclusion

The effects of ovariectomy on the murine tibia bone were quantified in two common mouse strains, using in vivo microCT and μFE modelling. The results of this study show strain-, time- and compartment-dependent changes in morphometric and densitometric properties, in particular persistent OVX-related trabecular bone loss and inhibition of cortical thickening in C57BL/6 that was not apparent or otherwise transient in BALB/c. These findings highlight the importance of choosing an appropriate mouse model for research of treatments against accelerated bone resorption. The differences in the bony response to OVX between the mouse strains suggest that BALB/c mice may be most useful in short-term and C57BL/6 useful in long-term investigations of anti-osteoporotic therapies. Future research should consider also the effects of OVX in old mice, with consideration for age-related changes and co-morbidities that are characteristic in the human disease.

Funding sources

This study was funded by the Engineering and Physical Sciences Research Council (EPSRC, Frontier Multisim Grant: EP/K03877X/1) and the UK National Centre for the Replacement, Refinement and Reduction of Animals in Research (NC3Rs, grant numbers: NC/K000780/1 and NC/R001073/1).

Declaration of Competing Interest

The authors report no conflicts of interest.

Acknowledgments

The authors thank Anne CM Fowles for technical assistance and the skelet.AL laboratory (http://skeletal.group.shef.ac.uk/) for access to the scanning facilities.

Appendix A. Supplementary data

Supplementary data to this article can be found online at https://doi.org/10.1016/j.bone.2019.06.024.

References

[1] O. Johnell, J.A. Kanis, An estimate of the worldwide prevalence and disability associated with osteoporotic fractures, Osteoporos. Int. 17 (12) (2006) 1726–1733.
[2] S.K. Boyd, P. Davison, R. Müller, J.A. Gasser, Monitoring individual morphological changes over time in ovariectomized rats by in vivo micro-computed tomography, Bone 39 (4) (2006) 854–862.
[3] J.E.M. Brouwers, B. van Rietbergen, R. Huiskes, K. Ito, Effects of PTH treatment on tibial bone of ovariectomized rats assessed by in vivo micro-CT, Osteoporos. Int. 20 (11) (2009) 1823–1835.
[4] E. Perilli, V. Le, B. Ma, P. Salmon, K. Reynolds, N.L. Fazzalari, Detecting early bone changes using in vivo micro-CT in ovariectomized, zoledronic acid-treated, and sham-operated rats, Osteoporos. Int. 21 (8) (2010) 1371–1382.
[5] M.L. Bouxsein, K.S. Myers, K.L. Shultz, L.R. Donahue, C.J. Rosen, W.G. Beamer, Ovariectomy-induced bone loss varies among inbred strains of mice, J. Bone Miner. Res. 20 (7) (2005) 1085–1092.
[6] R.L. Jilka, The relevance of mouse models for investigating age-related bone loss in humans, J. Gerontol. A 68 (10) (2013) 1209–1217.
[7] B. Roche, A. Vanden-Bossche, L. Malaval, M. Normand, M. Jannot, R. Chaux, L. Vico, M.-H. Lafage-Proust, Parathyroid hormone 1-84 targets bone vascular structure and perfusion in mice: impacts of its administration regimen and of ovariectomy, J. Bone Miner. Res. 29 (7) (2014) 1608–1618.
[8] S.K. Hui, G.R. Fairchild, L.S. Kidder, M. Sharma, M. Bhattacharya, S. Jackson, C. Le, D. Yee, Skeletal remodeling following clinically relevant radiation-induced bone damage treated with zoledronic acid, Calcif. Tissue Int. 90 (1) (2012) 40–49.
[9] T. Sugiyama, L.K. Saxon, G. Zaman, A. Moustafa, A. Sunters, J.S. Price, L.E. Lanyon, Mechanical loading enhances the anabolic effects of intermittent parathyroid hormone (1-34) on trabecular and cortical bone in mice, Bone 43 (2) (2008) 238–248.
[10] L.B. Meakin, H. Todd, P.J. Delisser, G.L. Galea, A. Moustafa, L.E. Lanyon, S.H. Windahl, J.S. Price, Parathyroid hormone's enhancement of bones' osteogenic response to loading is affected by ageing in a dose- and time-dependent manner, Bone 98 (2017) 59–67.
[11] S. Zhou, G. Wang, L. Qiao, Q. Ge, D. Chen, Z. Xu, D. Shi, J. Dai, J. Qin, H. Teng, Age-dependent variations of cancellous bone in response to ovariectomy in C57BL/6J mice, Exp. Ther. Med. 15 (4) (2018) 3623–3632.
[12] U.T. Iwaniec, D. Yuan, R.A. Power, T.J. Wronski, Strain-dependent variations in the response of cancellous bone to ovariectomy in mice, J. Bone Miner. Res. 21 (7) (2006) 1068–1074.
[13] Y. Li, M.B. Schaffler, H.T. Wolde-Semait, C.J. Hernandez, K.J. Jepsen, Genetic background influences cortical bone response to ovariectomy, J. Bone Miner. Res. 20 (12) (2005) 2150–2158.
[14] C. Deckard, A. Walker, B.J.F. Hill, Using three-point bending to evaluate tibia bone strength in ovariectomized young mice, J. Biol. Phys. 43 (1) (2017) 139–148.
[15] M.L. Bouxsein, S.K. Boyd, B.A. Christiansen, R.E. Guldberg, K.J. Jepsen, R. Müller, Guidelines for assessment of bone microstructure in rodents using micro–computed tomography, J. Bone Miner. Res. 25 (7) (2010) 1468–1486.
[16] E. Dall'Ara, M. Boudiffa, C. Taylor, D. Schug, E. Fiegle, A.J. Kennerley, C. Damianou, G.M. Tozer, F. Kiessling, R. Müller, Longitudinal imaging of the ageing mouse, Mech. Ageing Dev. 160 (2016) 93–116.
[17] G.M. Campbell, S. Tiwari, F. Grundmann, N. Purcz, C. Schem, C.-C. Glüer, Three-dimensional image registration improves the long-term precision of in vivo micro-computed tomographic measurements in anabolic and catabolic mouse models, Calcif. Tissue Int. 94 (3) (2014) 282–292.
[18] S.K. Boyd, S. Moser, M. Kuhn, R.J. Klinck, P.L. Krauze, R. Müller, J.A. Gasser, Evaluation of three-dimensional image registration methodologies for in vivo micro-computed tomography, Ann. Biomed. Eng. 34 (10) (2006) 1587–1599.
[19] F.M. Lambers, G. Kuhn, F.A. Schulte, K. Koch, R. Müller, Longitudinal assessment of in vivo bone dynamics in a mouse tail model of postmenopausal osteoporosis, Calcif. Tissue Int. 90 (2) (2012) 108–119.
[20] Y. Lu, M. Boudiffa, E. Dall'Ara, Y. Liu, I. Bellantuono, M. Viceconti, Longitudinal effects of parathyroid hormone treatment on morphological, densitometric and mechanical properties of mouse tibia, J. Mech. Behav. Biomed. Mater. 75 (2017) 244–251.
[21] M. Viceconti, E. Dall'Ara, From bed to bench: how in silico medicine can help ageing research, Mech. Ageing Dev. 177 (2018) 103–108.
[22] J. Klinck, S.K. Boyd, The magnitude and rate of bone loss in ovariectomized mice differs among inbred strains as determined by longitudinal in vivo micro-computed tomography, Calcif. Tissue Int. 83 (1) (2008) 70–79.
[23] Y. Lu, Y. Liu, C. Wu, J. Li, Investigating the longitudinal effect of ovariectomy on bone properties using a novel spatiotemporal approach, Ann. Biomed. Eng. 46 (5) (2018) 749–761.

[24] R.J. Klinck, G.M. Campbell, S.K. Boyd, Radiation effects on bone architecture in mice and rats resulting from in vivo micro-computed tomography scanning, Med. Eng. Phys. 30 (7) (2008) 888–895.
[25] K. Laperre, M. Depypere, N. van Gastel, S. Torrekens, K. Moermans, R. Bogaerts, F. Maes, G. Carmeliet, Development of micro-CT protocols for in vivo follow-up of mouse bone architecture without major radiation side effects, Bone 49 (4) (2011) 613–622.
[26] S. Reinwald, D. Burr, Review of nonprimate, large animal models for osteoporosis research, J. Bone Miner. Res. 23 (9) (2008) 1353–1368.
[27] R.D. Chapurlat, P. Garnero, E. Sornay-Rendu, M.E. Arlot, B. Claustrat, P.D. Delmas, Longitudinal study of bone loss in pre- and perimenopausal women: evidence for bone loss in perimenopausal women, Osteoporos. Int. 11 (6) (2000) 493–498.
[28] S.R. Cummings, J.S. Martin, M.R. McClung, E.S. Siris, R. Eastell, I.R. Reid, P. Delmas, H.B. Zoog, M. Austin, A. Wang, Denosumab for prevention of fractures in postmenopausal women with osteoporosis, N. Engl. J. Med. 361 (8) (2009) 756–765.
[29] P. Zysset, D. Pahr, K. Engelke, H.K. Genant, M.R. McClung, D.L. Kendler, C. Recknor, M. Kinzl, J. Schwiedrzik, O. Museyko, A. Wang, C. Libanati, Comparison of proximal femur and vertebral body strength improvements in the FREEDOM trial using an alternative finite element methodology, Bone 81 (2015) 122–130.
[30] G. Vaida, C. Ernesto, S. Lisa, M.L. B., Age-related changes in trabecular architecture differ in female and male C57BL/6J mice, J. Bone Miner. Res. 22 (8) (2007) 1197–1207.
[31] S. Oliviero, Y. Lu, M. Viceconti, E. Dall'Ara, Effect of integration time on the morphometric, densitometric and mechanical properties of the mouse tibia, J. Biomech. 65 (2017) 203–211.
[32] Y. Lu, M. Boudiffa, E. Dall'Ara, I. Bellantuono, M. Viceconti, Development of a protocol to quantify local bone adaptation over space and time: quantification of reproducibility, J. Biomech. 49 (10) (2016) 2095–2099.
[33] R.J. van't Hof, E. Dall'Ara, Analysis of bone architecture in rodents using micro-computed tomography, in: A.I. Idris (Ed.), Bone Research Protocols, Springer New York, New York, NY, 2019, pp. 507–531.
[34] S. Tassani, C. Öhman, F. Baruffaldi, M. Baleani, M. Viceconti, Volume to density relation in adult human bone tissue, J. Biomech. 44 (1) (2011) 103–108.
[35] S. Oliviero, M. Giorgi, E. Dall'Ara, Validation of finite element models of the mouse tibia using digital volume correlation, J. Mech. Behav. Biomed. Mater. 86 (2018) 172–184.
[36] Y. Chen, E. Dall'Ara, E. Sales, K. Manda, R. Wallace, P. Pankaj, M. Viceconti, Micro-CT based finite element models of cancellous bone predict accurately displacement once the boundary condition is well replicated: a validation study, J. Mech. Behav. Biomed. Mater. 65 (2017) 644–651.
[37] D.J. Webster, P.L. Morley, G.H. van Lenthe, R. Müller, A novel in vivo mouse model for mechanically stimulated bone adaptation – a combined experimental and computational validation study, Comput. Methods Biomech. Biomed. Engin. 11 (5) (2008) 435–441.
[38] H.H. Bayraktar, E.F. Morgan, G.L. Niebur, G.E. Morris, E.K. Wong, T.M. Keaveny, Comparison of the elastic and yield properties of human femoral trabecular and cortical bone tissue, J. Biomech. 37 (1) (2004) 27–35.
[39] U.T. Iwaniec, R.T. Turner, Failure to generate bone marrow adipocytes does not protect mice from ovariectomy-induced osteopenia, Bone 53 (1) (2013) 145–153.
[40] M. Almeida, S. Iyer, M. Martin-Millan, S.M. Bartell, L. Han, E. Ambrogini, M. Onal, J. Xiong, R.S. Weinstein, R.L. Jilka, Estrogen receptor-α signaling in osteoblast progenitors stimulates cortical bone accrual, J. Clin. Invest. 123 (1) (2012).
[41] Y. Tajima, S. Yokose, M. Kawasaki, T. Takuma, Ovariectomy causes cell proliferation and matrix synthesis in the growth plate cartilage of the adult rat, Histochem. J. 30 (7) (1998) 467–472.
[42] H.G. Ahlborg, O. Johnell, C.H. Turner, G. Rannevik, M.K. Karlsson, Bone loss and bone size after menopause, N. Engl. J. Med. 349 (4) (2003) 327–334.
[43] K.L. Beaucage, S.I. Pollmann, S.M. Sims, S.J. Dixon, D.W. Holdsworth, Quantitative in vivo micro-computed tomography for assessment of age-dependent changes in murine whole-body composition, Bone Rep. 5 (2016) 70–80.
[44] T.A. Damron, B.S. Margulies, J.A. Strauss, K. O'hara, J.A. Spadaro, C.E. Farnum, Sequential histomorphometric analysis of the growth plate following irradiation with and without radioprotection, JBJS 85 (7) (2003) 1302–1313.
[45] T. Mustafy, A. Benoit, I. Londono, F. Moldovan, I. Villemure, Can repeated in vivo micro-CT irradiation during adolescence alter bone microstructure, histomorphometry and longitudinal growth in a rodent model? PLoS One 13 (11) (2018) e0207323.
[46] J.H. Waarsing, J.S. Day, J.C. van der Linden, A.G. Ederveen, C. Spanjers, N. De Clerck, A. Sasov, J.A.N. Verhaar, H. Weinans, Detecting and tracking local changes in the tibiae of individual rats: a novel method to analyse longitudinal in vivo micro-CT data, Bone 34 (1) (2004) 163–169.
[47] I.M. Sigrist, C. Gerhardt, M. Alini, E. Schneider, M. Egermann, The long-term effects of ovariectomy on bone metabolism in sheep, J. Bone Miner. Metab. 25 (1) (2007) 28–35.
[48] F. Callewaert, K. Venken, J.J. Kopchick, A. Torcasio, G.H. Lenthe, S. Boonen, D. Vanderschueren, Sexual dimorphism in cortical bone size and strength but not density is determined by independent and time-specific actions of sex steroids and IGF-1: evidence from pubertal mouse models, J. Bone Miner. Res. 25 (3) (2010) 617–626.
[49] K.B. Emerton, B. Hu, A.A. Woo, A. Sinofsky, C. Hernandez, R.J. Majeska, K.J. Jepsen, M.B. Schaffler, Osteocyte apoptosis and control of bone resorption following ovariectomy in mice, Bone 46 (3) (2010) 577–583.
[50] G. Osterhoff, E.F. Morgan, S.J. Shefelbine, L. Karim, L.M. McNamara, P. Augat, Bone mechanical properties and changes with osteoporosis, Injury 47 (2016) S11–S20.
[51] M.A. Brennan, J.P. Gleeson, F.J. O'Brien, L.M. McNamara, Effects of ageing, prolonged estrogen deficiency and zoledronate on bone tissue mineral distribution, J. Mech. Behav. Biomed. Mater. 29 (2014) 161–170.
[52] M.J. Silva, M.D. Brodt, B.A. Uthgenannt, Morphological and mechanical properties of caudal vertebrae in the SAMP6 mouse model of senile osteoporosis, Bone 35 (2) (2004) 425–431.
[53] A.I. Birkhold, H. Razi, G.N. Duda, R. Weinkamer, S. Checa, B.M. Willie, The influence of age on adaptive bone formation and bone resorption, Biomaterials 35 (34) (2014) 9290–9301.